Synthesis and Characterization of Nanofibrous Sodium Manganese Oxide with a 2 × 4 Tunnel Structure

Guan-Guang Xia,[†,‡] Wei Tong,[‡] Elaine N. Tolentino,[‡,||] Nian-Gao Duan,[†,‡,⊥] Stephanie L. Brock,[‡,#] Jin-Yun Wang,[‡] and Steven L. Suib*[,†,‡,§]

Institute of Materials Science and Departments of Chemistry and Chemical Engineering, The University of Connecticut, Storrs, Connecticut 06269

Thorsten Ressler

Fritz-Haber Institut der MPG, Berlin, Germany

Received September 27, 2000. Revised Manuscript Received February 9, 2001

Sodium manganese oxide octahedral molecular sieves with a 2 × 4 tunnel structure (Na−2 × 4) have been hydrothermally synthesized from Na−birnessite materials at low temperatures and pressures. The synthetic template materials, the pH value of the medium, and the autoclaved temperature are critical in the synthesis. Sodium salts, such as NaCl, $NaNO_3$, and Na_2SO_4, are good templates for Na−2 × 4. In strong basic solution or below 160 °C, Na−birnessite does not transform to the Na−2 × 4 structure. TEM images show the synthesized Na−2 × 4 is made up of thin slablike single crystals elongated along the *b* axis. The formula of Na−2 × 4 can be written as $Na_{0.33}Mn^{3+}_{0.33}Mn^{4+}_{0.67}O_2{\cdot}xH_2O$, and it is monoclinic with space group *C*2/*m*. The unit cell parameters (*a*, *b*, *c*, and β) for Na−2 × 4 are 14.434(5) Å, 2.849(7) Å, 23.976(6) Å, and 98.18°, respectively. These data for Na−2 × 4 are slightly different from the data for Rb−2 × 4 synthesized under high pressure and high temperature, which were reported by Rziha et al. (*Eur. J. Miner.* **1996**, *8*, 1155−1161). The surface area of Na−2 × 4 is about 57 m^2/g. Na−2 × 4 materials are thermally stable up to 450 °C as indicated by TGA and TPD data.

I. Introduction

Both natural and synthetic microporous manganese oxides have been intensively investigated for several decades because of their economic value and potential application as molecular sieves in catalysis and cathodes in batteries.[1] These manganese oxide structures are built of manganese oxide octahedra [MnO_6] sharing their edges and corners to form one-dimensional tunnel structures of various sizes. These materials are mixed valent with oxidation states of manganese of 4, 3, or 2. The general formula can be written as A_xMnO_2, where A represents the cations, which are accommodated in the tunnels to support the framework and to maintain charge balance.

The microporous manganese oxides can be classified into three groups[2] based on the number of MnO_6 octahedral chains between two basal layers to form tunnel openings (Figure 1). The 1 × *n* group includes pyrolusite (with a 1 × 1 tunnel) [3] and ramsdellite (1 × 2).[4] The 2 × *n* group consists of hollandite (2 × 2),[5] romanechite (2 × 3),[6,7] RUB-7 (Rb−2 × 4),[8] and $Rb_{0.27}MnO_2$ (2 × 5).[9] Todorokite (3 × 3)[10] is a member of the 3 × *n* group.

Rziha and colleagues first reported a new synthetic manganese oxide with a 2 × 4 tunnel structure (RUB-7).[11] These porous crystalline materials were synthesized by hydrothermal treatment of alkali-birnessite in hydroxide solutions at 350 °C and 2 kbar using a gold capsule. The Rietveld refinement of Rb−RUB-7 gave a monoclinic space group with lattice parameters a = 14.193(3) Å, b = 2.851(1) Å, c = 24.343(7) Å, and β = 91.29(2)°. The ideal formula for Rb−RUB-7 was reported as $Rb_{0.67}MnO_2$. However, because only small amounts of samples were available, the authors could not do chemical analyses and further characterization. No

* To whom correspondence should be addressed.
† Institute of Materials Science, The University of Connecticut.
‡ Department of Chemistry, The University of Connecticut.
§ Department of Chemical Engineering, The University of Connecticut.
|| Current address: Department of Chemistry, De La Salle University, Philippines.
⊥ Current address: Department of Chemistry, Wayne University.
Current address: Department of Chemistry, Oregon State University.

(1) Suib, S. L. *Curr. Opin. Solid State Mater. Sci.* **1998**, *3* (1), 63−70.
(2) Turner, S.; Buseck, P. R. *Science* **1981**, *212*, 1024−1027.
(3) Baur, W. H. *Acta Crystallogr.* **1976**, *B32*, 2200−2204.
(4) Byström, A. M. *Acta Chem. Scand.* **1949**, *3*, 163−173.
(5) Byström, A.; Byström, A. M. *Acta Crystallogr.* **1950**, *3*, 146−154.
(6) Wadsley, A. D. *Acta Crystallogr.* **1953**, *6*, 433−438.
(7) Turner, S.; Post J. E. *Am. Mineral.* **1988**, *73*, 1155−1161.
(8) Rziha, T.; Gies, H.; Rius, J. *Eur. J. Mineral.* **1996**, *8*, 675−686.
(9) Tamada, O. and Yamamoto, N., *Mineral. J.* **1986**, *13* (3), 130−140.
(10) Burns, R. G.; Burns, V. M.; and Stockman, H. W., *Am. Mineral.* **1983**, *68*, 972−980.
(11) Rziha, T.; Gies, H.; Rius, J. *Eur. J. Mineral.* **1996**, *8*, 675−686.

10.1021/cm000777r CCC: $20.00
Published on Web 04/05/2001

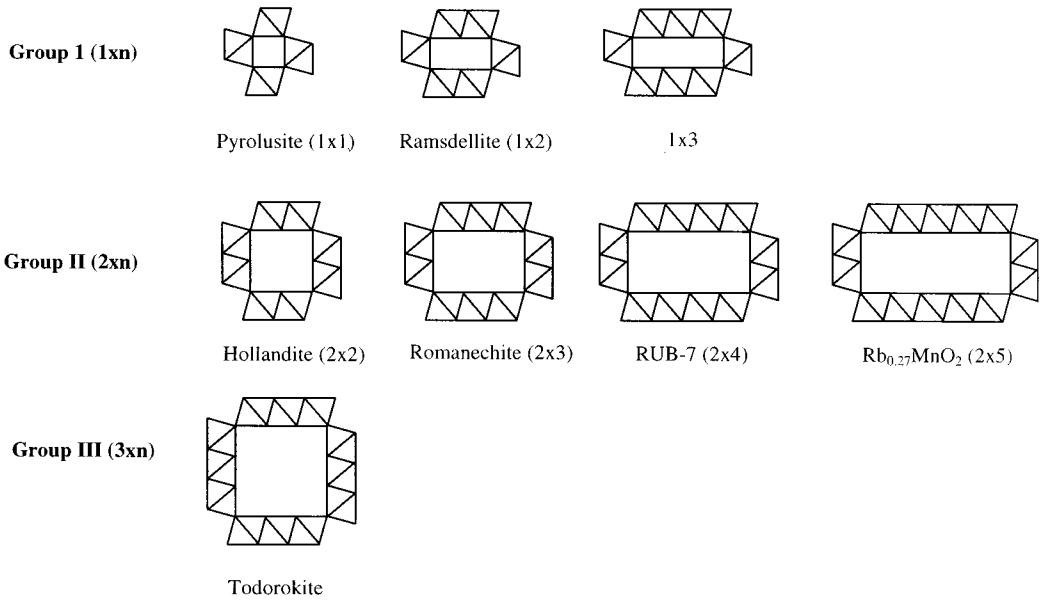

Figure 1. Schematic drawings of manganese oxides with different tunnel openings.

other physical or chemical properties for this material have been reported so far. In this article, we report a new approach to synthesize Na−2 × 4 materials at low temperatures and low pressures by a hydrothermal method. Some structural properties of the Na−2 × 4 materials are also studied here. Earlier work concerning catalysis with this system has been presented elsewhere.[12,13]

II. Experimental Section

1. Synthesis. Na−2 × 4 materials are hydrothermally synthesized using Na−birnessite materials as precursors at low temperature (180−240 °C) and autogenous pressure. Several synthetic methods for preparing birnessite have been reported in the literature.[14−18] In this work, Na−birnessite was synthesized by a redox reaction between Mn(VII) and Mn(II) in basic media at room temperature. Solution A (100 mL), which contains 5.62 g of $MnCl_2 \cdot 4H_2O$ was added dropwise into another 100 mL of solution B, which consists of 1.58 g of $KMnO_4$ and 12 g of NaOH while being stirred vigorously. A black precipitate was formed. The precipitate was aged for 1 day at room temperature before it was separated from the solution. The precipitate (Na−birnessite) was washed several times with distilled deionized water (DDW) until the pH reached 8.

About 5 g of wet Na−birnessite samples and 10 mL of 5 M NaCl solution (or other Na^+ sources, such as $NaNO_3$ and Na_2SO_4) were sealed in a 30-mL autoclave with a Teflon liner and the autoclave was heated at 180−240 °C for 2 days. The gray-black solids were thoroughly washed with DDW. The samples were then dried at 110 °C overnight prior to characterization. Besides sodium salts, other cation sources were also employed to replace Na^+, including Li^+, K^+, Rb^+, NH_4^+, Ca^{2+}, and Mg^{2+}.

2. XRD Pattern and SEM/TEM Analysis. Powder X-ray diffraction (XRD) data were collected with a Scintag 2000 PDS X-ray diffractometer using Cu Kα radiation (1.54060 A). Samples were well ground in acetone and then packed on a side-slitted aluminum sample holder using a side-packing technique to minimize preferred orientation effects. A set of slits with widths of 1, 2, 0.5, and 0.3 mm were used as the emitter and receiver slits, respectively. The beam voltage was 45 kV and the beam current was 40 mA. The step scan rate was 15 s/step and step size was 0.02° (2θ). The instrument was calibrated using a standard LaB_6 crystal sample prior to powder X-ray diffraction analysis. The SEM image was obtained with an AMRAY Model 1810D scanning electron microscope. A tungsten filament was used as an electron source and the acceleration potential was 25 kV.

Powdered Na−2 × 4 samples were well ground before being dispersed in acetone under ultrasonic conditions. Fine particles were placed on a carbon-coated Cu grid for TEM measurements. The TEM images and electron diffraction patterns were obtained with a Philips EM-420 analytical electron microscope.

3. Elemental Analysis and Average Oxidation State Determination. The quantitative analysis of sodium and manganese were carried out with a Perkin−Elmer Model 140 ICP-AES system.

A potential voltametric titration method was developed to determine the average oxidation states of manganese in the samples. The titration method includes two steps. The first step involves determining the total amount of manganese in the sample. A 10−20-mg sample with 2 mL of concentrated hydrochloride acid was added to a 50-mL Erlenmeyer flask covered with a watch glass. The samples were dissolved completely and the resulting solution was transferred into a 100-mL volumetric flask and diluted to the 100-mL mark with DDW. The diluted solution (25 mL) and 50 mL of the saturated sodium pyrophosphate solution were then added into a 200-mL beaker. When the pH value of the system reached about 7 when adjusted with a 1 M NaOH solution, the system was titrated with a 1×10^{-3} M potassium permanganate solution. The potential change (in mV) of the system during the course of titration was monitored with a Fisher Scientific Accumet pH meter 25 (at mV position) with a pair of electrodes (Calomel and Pt). The reactions involved in this step are

(12) Xia, G. G.; Wang, J, Y.; Ma, Y.; Duan, N. G.; Suib, S. L. *Shape Selective Catalysis*: *Chemicals Synthesis and Hydrocarbon Processing*; Song, C. S., Garces, J. M., Sugi, Y., Eds.; American Chemical Society: Washington, D.C., 1999; Chapter 6, pp 80−93.

(13) Xia, G. G.; Wei, T.; Elaine, N. T.; Brock, S. L.; Duan, N. G.; Suib, S. L. *Book of Abstracts*, 219th ACS National Meeting, San Francisco, CA, March 26−30, 2000.

(14) Golden, D. C.; Chen, C. C.; Dixon, J. B. *Science* **1986**, *231* (4739), 717−19.

(15) Bach, S.; Pereira-Ramos, J. P.; Baffier, N.; Messina, R. *Electrochim. Acta* **1991**, *36* (10), 1595−1603.

(16) Shen, Y. F.; Zerger, R. P.; Suib, S. L.; McCurdy, L.; Potter, D. I.; O'Young, C. L., *J. Chem. Soc., Chem. Commun.* **1992**, (17), 1213−14.

(17) Suib, S. L.; O'Young, C. L. *Synthesis of Octahedral Molecular Sieves and Layered Materials*; Chem. Ind. (Dekker): New York, 1997; Vol. 69 (Synthesis of Porous Materials), pp 215−231.

(18) Aronson, B. J.; Kinser, A. K.; Passerini, S.; Smyrl, W. H.; Stein, A. *Chem. Mater.* **1999**, *11* (4), 949−957.

$$MnO_2^{x-}(s) + (2 - x)Cl(aq) + 4H^+(aq) \rightleftarrows Mn^{2+}(aq) + (1 - x/2)Cl_2(g) + 2H_2O(l) \quad (1)$$

$$MnO_4^-(aq) + 4Mn^{2+}(aq) + 15H_2P_2O_7^{2+}(aq) + 8H^+(aq) \rightleftarrows 5Mn(H_2P_2O_7)_3^{3-}(aq) + 4H_2O(l) \quad (2)$$

The total Mn in the sample can be calculated using the following equation:

$$M_{Mn} = 4 \times C_{KMnO_4} \times V_1/W_1 \text{ (mol/g)} \quad (3)$$

where C_{KMnO_4} is the concentration (in mol/L) of $KMnO_4$ solution, V_1 is the volume (in L) of the consumed $KMnO_4$ solution, and W_1 is the weight (in g) of the sample, respectively.

The second step involves measuring the amount of manganese with oxidation states over 2. About 20-mg samples were weighed and transferred into a 100-mL Erlenmeyer flask and 10 mL of 0.05 M $(NH_4)_2Fe(SO_4)_2$ was added. When all solids were dissolved, the solution was titrated with the potassium permanganate solution. A sharp purple color appears when the titration reaches the end point. Equations 4 and 5 describe these reactions:

$$MnO_2^{(4-n)-}(s) + (n - 2)Fe^{2+}(aq) + 4H^+(aq) \rightleftarrows (n - 2)Fe^{3+}(aq) + Mn^{2+}(aq) + 2H_2O(l) \quad (4)$$

$$MnO_4^-(aq) + 5Fe^{2+}(aq) + 8H^+(aq) \rightleftarrows Mn^{2+}(aq) + 5Fe^{3+}(aq) + 4H_2O(l) \quad (5)$$

Because 1 mol of MnO_4^- is equivalent to $5/(n - 2)$ mol of Mn^{n+}, the total amount of Mn in the sample can be calculated in this step using eq 6,

$$M_{Mn} = 5/(n - 2)C_{KMnO_4}(V_2 - V_3)/W_2 \quad (6)$$

where n is the average oxidation state (AOS) of Mn in the sample, C_{KMnO_4} is the concentration of the $KMnO_4$ solution, V_2 is the volume of $KMnO_4$ solution for blank titration, V_3 is the volume of consumed $KMnO_4$ solution for the titration of the sample, and W_2 is the weight of the sample in the second step.

Combining eqs 3 and 6, the AOS of the sample can be calculated by eq 7:

$$n = 1.25 \times (V_2 - V_3)/V_1 \times W_1/W_2 \quad (7)$$

4. Thermogravimetric Analysis (TGA) and Temperature-Programmed Desorption (TPD). TGA data were collected with a TA Instrument Model 2950. The experiments were conducted under a N_2 atmosphere (10 mL/min) and the temperature was increased from ambient to 900 °C at a ramp rate of 10 °C/min.

TPD analysis was done with a lab-made setup. Samples (~20 mg) were placed into a quartz tube with a sintered glass filter. The samples were heated in flowing He from room temperature to 750 °C at 10 °C/min controlled with a programmable temperature controller (OMEGA). The evolved materials were screened with a MKS-UTI PPT quadrupole mass spectrometer.

5. Specific Surface Area Measurement. A Micromeritics ASAP 2010 accelerated surface area and porosimetry system was employed for the specific surface area measurement. Nitrogen gas was used as an adsorbate at 77 K. The samples were pre-degassed at 250 °C for 12 h and purged with He. The specific surface area of a sample was measured using a BET method.

6. Extended X-ray Absorption Fine Structure (EXAFS). EXAFS experiments were performed at Stanford Synchrotron Radiation Laboratory (SSRL) with the storage ring operating at the energy of 3.0 GeV and injection current of about 100 mA.[19] An equivalent step size of 1.0 eV/point was used for the EXAFS scans. A piece of manganese metal foil was placed in front of the reference ion chamber and measured simultaneously with the sample in question for energy calibration.

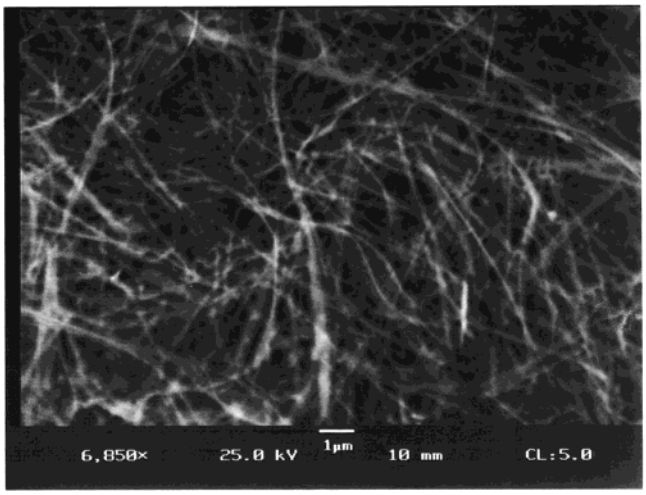

Figure 2. SEM image of Na−2 × 4. The materials show nanofibrous morphology.

III. Results

1. Synthesis. Under synthetic conditions similar to those mentioned in the Experimental Section, Na−birnessite incorporated with different cations, including Li^+, Na^+, K^+, NH_4^+, Rb^+, Ca^{2+}, and Mg^{2+}, gave different results. Interestingly, only Na-rich birnessite yields good quality Na−2 × 4 while other cations lead to the formation of new phases. For example, Li^+, NH_4^+, and Mg^{2+} lead to spinel, 2 × 2, and 3 × 3 structures, respectively. These will be discussed elsewhere.

Besides cation template effects, temperature and pressure are definitely also very important for the transformation. There was no significant change of the Na-saturated birnessite heated at 160 °C for 10 days in an autoclave. In the range 180−240 °C, the Na−birnessites were converted to Na−2 × 4 materials to different extents. As the experimental temperature was elevated, the extent of conversion increased.

2. Crystal Structure Analysis. The synthesized sodium manganese oxides are black nanofibers (see the SEM image of Figure 2). The average thickness of the fibers is about 60 nm. X-ray diffraction data are shown in Figure 3. The first peak appears at a d spacing of about 12 Å. The peak indexing results are summarized in Table 1.

A TEM image and a corresponding electron diffraction pattern (ED) of the fibrous Na−2 × 4 are shown in Figure 4. The spacing in the fringes of the TEM image is about 12 Å, which is half of the c axis (~24 Å). The ED pattern in the single crystal gives b and c values of the unit cell, which are about 2.85 and 12 Å ($^1/_2c$), respectively.

The elemental analysis and titration data indicate that the synthesized material has a formula in one unit cell of $Na_8Mn_{24}O_{48}{\cdot}xH_2O$. The average oxidation state of manganese oxide is 3.67.

(19) Ma, Y.; Suib, S. L.; Ressler, T.; Wong, J.; Lovallo, M.; Tsapatsis, M. *Chem. Mater.* **1999**, *11*, 3545−3554.

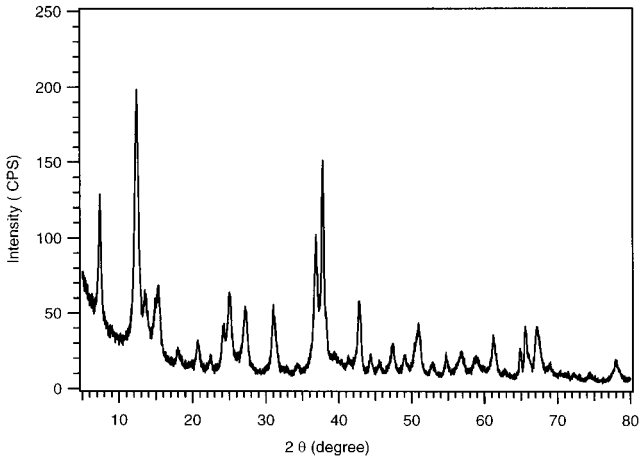

Figure 3. X-ray diffraction pattern of Na−2 × 4.

3. Thermal Stability. The TGA curves for Na−2 × 4 and Na−birnessite are shown in Figure 5, parts a and b, respectively. The weight loss at 350 °C was about 6% for Na−2 × 4. The derivative profiles of the TGA curves show two peaks under 350 °C for Na−2 × 4 and three peaks between 450 and 900 °C. However, the weight loss of Na−birnessite is about 10%.

The TPD profiles of Na−2 × 4 materials for the removal of O_2 and adsorptive carbon dioxide are shown in Figure 6a. To compare with the profile of Na−2 × 4, the TPD profiles of Na−birnessite are shown in Figure 6b. Because water vapor was strongly adsorbed on the wall of the sample tube and the inlet tube of the TPD-MS, water peaks are not well-resolved and are not shown in the figures.

According to the TGA and TPD data for Na−2 × 4, the materials removed under 350 °C are mainly water and small amounts of adsorptive gases, such as CO_2. The first peak at about 150 °C in the TGA derivative profile may be related to adsorbed water on Na−2 × 4 materials and the second peak may be the result of crystalline water or adsorbed water in the tunnels. These water peaks can be identified by in situ temperature-programmed FTIR analysis.[20] The three peaks above 350 °C indicate that removal of oxygen in the sample takes place as the temperature was elevated.

4. BET Surface Analysis. The isothermal plots of Na−2 × 4 are shown in Figure 7, which indicates microporous character. The BET surface area of Na−2 × 4 is 57.43 ± 0.36 m^2/g.

5. EXAFS Analysis. EXAFS spectroscopy is a very useful technique for obtaining structural information for the solid samples. The radial distribution function (RDF) derived from EXAFS at Mn−K edges can provide information about the surroundings of the local manganese ions. The radial distribution curve obtained by Fourier transformation of the EXAFS spectrum for Na−2 × 4 is shown in Figure 8. The curve is not phase-shift-corrected and hence the peak positions in the curve are shifted to lower R values by about 0.4 Å. [21] The peaks at 1.6, 2.3, and 3.1 Å are assigned to the average interatomic distances of Mn−O, Mn−Mn (edge-sharing octahedra), and Mn−Mn (corner-sharing octahedra), respectively. The peak at 3.1 Å is not found in Na−birnessite EXAFS spectra. EXAFS refinement with a suitable model can provide detailed interatomic distances between manganese atoms and their neighbors.

Table 1. X-ray Peak Indexing of Na−2 × 4

no.	h	k	l	$2\theta_{obs.}$	$2\theta_{calc.}$	$2\theta_{resid.}$	$d_{obs.}$(Å)
1	0	0	2	7.372	7.444	−0.072	11.922
2	2	0	0	12.366	12.378	−0.012	7.130
3	−2	0	2	13.501	13.514	−0.012	6.535
4	0	0	4	14.878	14.919	−0.041	5.935
5	2	0	2	15.289	15.347	−0.058	5.776
6	2	0	4	20.769	20.760	0.009	4.266
7	0	0	6	22.410	22.459	−0.048	3.957
8	−2	0	6	24.120	24.095	0.025	3.681
9	4	0	0	25.015	24.903	0.112	3.551
10	4	0	2	27.139	27.049	0.090	3.278
11	2	0	6	27.336	27.258	0.078	3.255
12	0	0	8	30.024	30.098	−0.074	2.970
13	−2	0	8	30.915	30.922	−0.007	2.887
14	4	0	4	30.976	30.978	−0.002	2.881
15	−4	0	6	31.309	31.230	0.079	2.851
16	1	1	2	33.137	33.106	0.031	2.698
17	2	0	8	34.222	34.297	−0.075	2.615
18	4	0	6	36.052	36.171	−0.102	2.487
19	3	1	0	36.719	36.718	0.001	2.443
20	3	1	1	37.228	37.204	0.025	2.411
21	6	0	0	37.777	37.740	0.037	2.377
22	−2	0	10	38.214	38.186	0.028	2.351
23	3	1	3	39.218	39.317	−0.098	2.293
24	6	0	2	39.567	39.610	−0.043	2.274
25	3	1	−5	40.134	40.194	−0.059	2.243
26	−1	1	7	41.716	41.251	−0.076	2.188
27	6	0	6	41.338	41.338	0.000	2.180
28	2	0	10	41.657	41.743	−0.086	2.164
29	1	1	7	42.355	42.450	−0.095	2.130
30	3	1	5	42.757	42.780	−0.022	2.111
31	6	0	4	42.864	42.848	−0.002	2.107
32	−3	1	7	44.064	44.004	0.059	2.052
33	−6	0	8	45.254	45.267	−0.013	2.000
34	6	0	6	47.278	47.229	0.049	1.919
35	4	0	10	48.934	48.968	−0.034	1.858
36	−8	0	2	50.415	50.536	−0.121	1.807
37	5	1	5	50.869	50.874	−0.005	1.792
38	8	0	0	51.135	51.092	0.044	1.783
39	−8	0	4	51.314	51.225	0.089	1.778
40	8	0	2	52.875	52.864	0.010	1.729
41	−2	0	14	53.756	53.720	0.036	1.703
42	8	0	8	56.146	56.149	−0.003	1.636
43	−7	1	5	56.705	56.640	0.065	1.621
44	8	0	6	59.720	59.709	0.019	1.543
45	7	1	5	61.211	61.211	0.000	1.514
46	1	1	13	61.406	61.375	0.031	1.508
47	0	0	16	62.660	62.570	0.090	1.480
48	10	0	4	64.762	64.847	−0.086	1.437
49	0	2	0	65.509	65.445	0.063	1.423
50	2	0	16	66.073	66.076	−0.003	1.412
51	2	2	1	67.141	64.157	−0.016	1.392
52	0	2	4	67.564	67.552	0.012	1.384
53	1	1	15	66.881	68.955	−0.074	1.361
54	2	2	4	69.463	69.474	−0.011	1.351
55	7	1	9	70.387	70.385	0.002	1.336
56	−4	2	1	71.059	71.067	−0.008	1.325
57	−4	2	4	72.240	72.253	−0.012	1.306
58	4	2	4	74.245	74.162	0.083	1.276
59	9	1	7	77.449	77.458	−0.009	1.231
60	0	2	10	78.204	78.151	0.053	1.220

IV. Discussion

1. The Transformation of Na−Birnessite to Na−2 × 4. Synthetic Na−birnessite (Na−OL) is a layered manganese oxide formed by edge-sharing MnO_6 octa-

(20) Xia, G. G.; Suib, S. L. Unplublished data.
(21) Ressler, T.; Brock, S. L.; Wong, J.; Suib, S. L. *J. Phys. Chem. B* **1999**, *103*, 6407−6420.

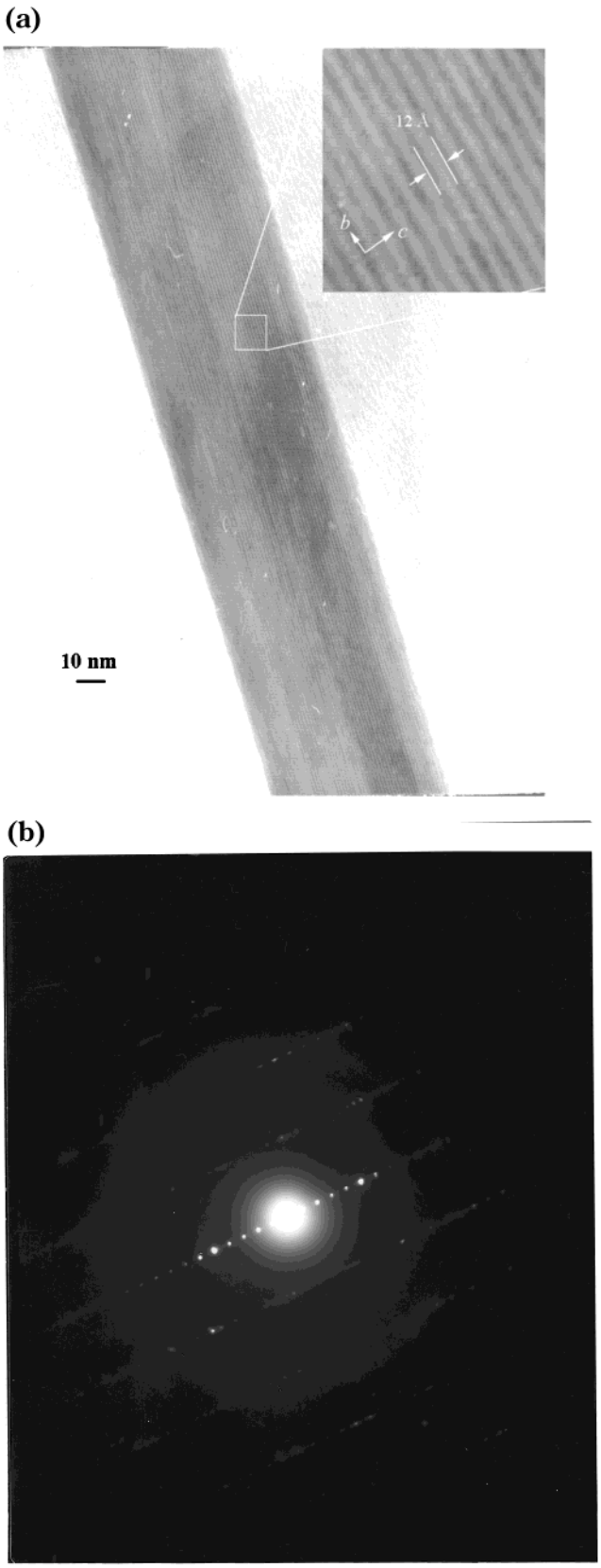

Figure 4. (a) TEM image of Na−2 × 4. The insert is the enlarged image. It clearly shows a distance of 12 Å between fringes, which reflects the half-length of the *c* axis of a unit cell. (b) ED pattern of a single-crystal Na−2 × 4. The two cell parameters, *b* and *c*, can be measured and calculated from the pattern.

hedra. Recently, Manceau, Drits, and colleagues[22,23] studied the Na−OL structure in detail and they concluded that Na−OL contained mixed Mn(IV) and Mn(III) octahedral layers in which every third row in the [010] direction primarily contains Mn^{3+}. The layer-layer stabilization of Na−OL must be retained by offsetting the excess negative charge with Na^+ in the layers, associated to some extent with hydrogen bonding between layer O atoms and interlayer H_2O molecules.

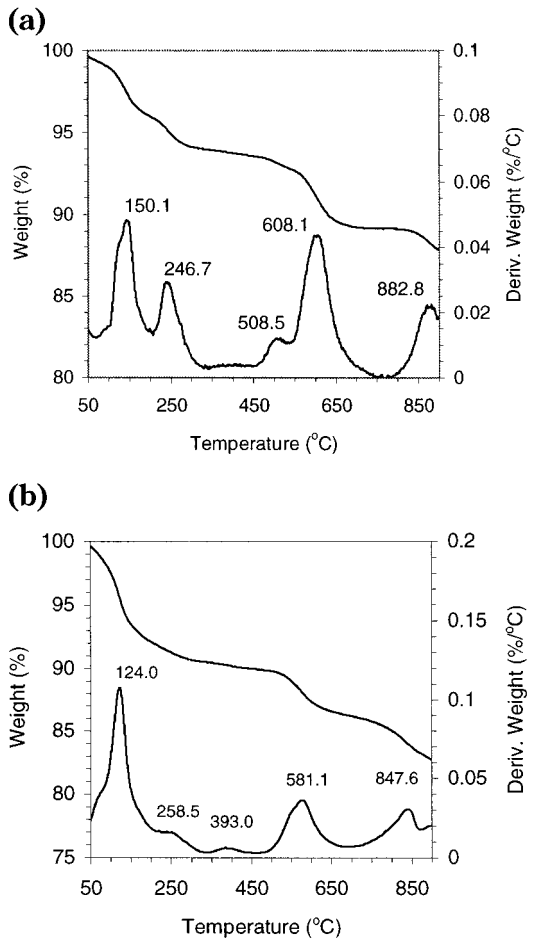

Figure 5. (a) TGA profile of Na−2 × 4. (b) TGA profile of Na−birnessite. In each profile, the first two peaks of the bottom plot (derivative of weight loss vs temperature) are assigned as absorbed and lattice water, respectively. The other peaks are related to loss of oxygen from the samples.

Starting from layered manganese oxide materials (OL-1), different manganese oxides with various tunnel structures have been synthesized,[24,25] such as OMS-1 (with a 3 × 3 tunnel),[26] OMS-2 (2 × 2),[27] and RUB-7 (2 × 4). The transformation of Na−OL to tunnel-structured manganese oxides under hydrothermal conditions is still not clear. The slight increase in the average oxidation state of manganese from 3.57 (Na−birnessite) to 3.67 (Na−2 × 4) during the course of transformation may

(22) Drits, V. A.; Silvester, E.; Gorshkov, A. I.; Manceau, A. *Am. Mineral.* **1997**, *82*, 946−961.
(23) Silvester, E.; Manceau, A.; Drits, V. A. *Am. Mineral.* **1997**, *82*, 962−978.
(24) Brock, S. L.; Duan, N. G.; Tian, Z. R.; Giraldo, O.; Hua, Z.; Suib, L. S. *Chem. Mater.* **1998**, *10*, 2619−2628.
(25) Feng, Q.; Yanagisawa, K.; Yamasaki, N. *Chem. Commun.* **1996**, 1607−1608.
(26) Shen, Y. F.; Zerger, R. P.; DeGuzman, R. N.; Suib, S. L.; McCurdy, L.; Potter, D. I.; O'Young, C. L. *Science* **1993**, *260*, 511−515.
(27) Chen, C.; Golden, D. C.; Dixon, J. B. *Clays Clay Miner.* **1986**, *34* (5), 565−571.

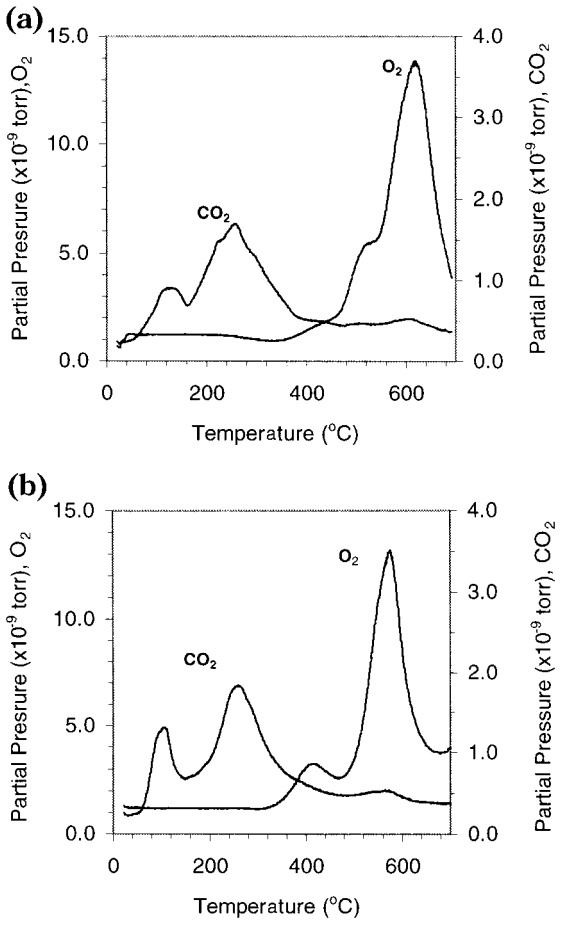

Figure 6. (a) TPD profile of Na−2 × 4. A significant amount of oxygen species is evolved above 450 °C. (b) TPD profile of Na−birnessite. The oxygen species are evolved at lower temperatures compared to data for Na−2 × 4.

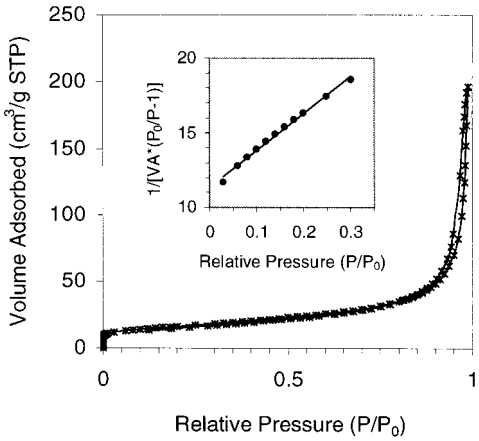

Figure 7. Isothermal plots of Na−2 × 4. N_2 at 77 K was used as a single absorbate. The lower pressure dose was set to 0.2 cm^3/g. Insert is the BET surface area plot.

indicate that very few lower valance manganese cations (Mn^{3+}) in the layers may be subjected to disproportionation according to the sequence in eq 8

$$Mn^{3+}_{layer} + Mn^{3+}_{layer} \rightarrow Mn^{4+}_{layer} + Mn^{2+}_{layer} \rightarrow Mn^{4+}_{layer} + \text{vacancy} + Mn^{2+}_{aq} \quad (8)$$

or are further oxidized by free oxygen in the autoclave. According to Manceau's suggestion, some Mn^{3+} may

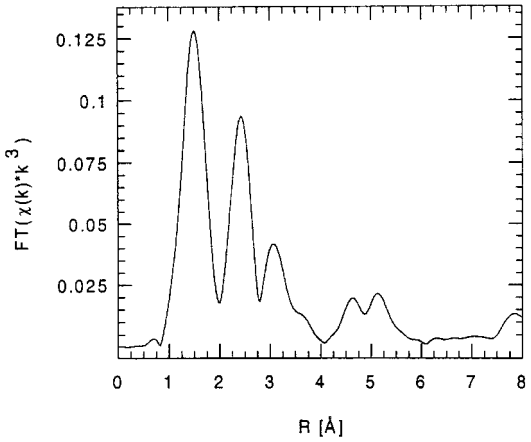

Figure 8. Radial distribution curve derived from the EXAFS spectrum of Na−2 × 4. The curve is not corrected for phase shift.

migrate into the interlayers and assist in the formation of corner-sharing manganese octahedra. The changes in Mn^{3+} cations will release steric strain due to Jahn−Teller distortion of these $Mn^{3+}O_6$ octahedra, thus decreasing the free energy of the system.

This transformation should be an endothermic process because it essentially involves bond dissociation steps. These processes are accelerated by an increase in autoclave temperature and pressure. At a lower temperature (160 °C), Na−birnessite samples still retain a layered structure and no significant amounts of tunnel structure materials were observed. As the autoclave temperature was elevated from 160 to 180 °C and above, the degree of transformation increased greatly. The fact that some condensed phases were observed at 240 °C might suggest that autogenous pressure was too high for this transformation process. Autoclave temperatures in the 200−230 °C range are ideal for Na−2 × 4 formation.

On the other hand, the kind of incorporated cations, anions, as well as the amount of water between the layers of birnessites play a key role as templates for the transformation from birnessites to different manganese oxides. Although it is still not well understood how the templates work in these transformation processes, the charge, the size (with associated water), and other chemical properties of the cation template are important for the conversion. Certain amounts of water may provide a medium for the separation of the cations from each other.

The Na−2 × 4 has a similar *d* spacing of 7 Å in the [2 0 0] direction with Na−birnessite in the [1 0 0] direction (the unit cell of Na−2 × 4 is doubled). The experimental results show that Na^+ is a suitable cation for the transformation from a layered birnessite to tunnel structure Na−2 × 4. In a similar case for hydrothermal synthesis of OMS-1 (3 × 3 tunnel), Mg^{2+} ion-exchanged Na−birnessite, which is called buserite, transformed to OMS-1 with both having a similar *d* spacing of 10 Å. Although Rb^+ has been reported as a template in the synthesis of Rb−2 × 4 at 350 °C and 2 kbar, Na^+ ion at these lower temperatures is a far better template. Probably the Rb^+ cations are too large for a template under such mild conditions.

At a relatively wide range of pH values from 7 to 11, good quality Na−2 × 4 can be obtained from Na−

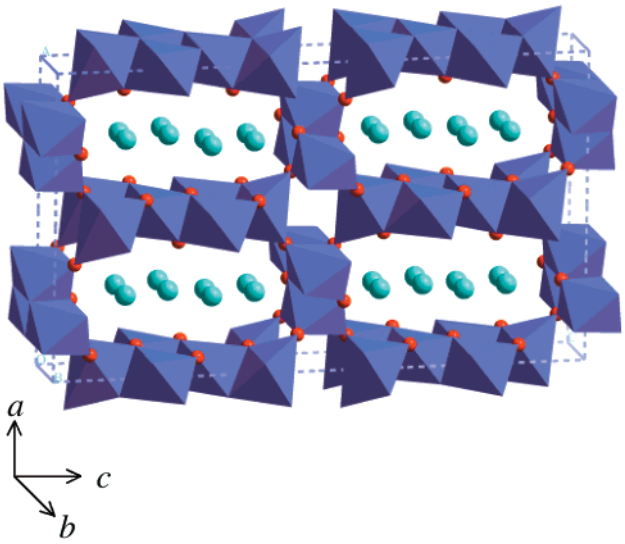

Figure 9. A model of Na−2 × 4. The isolated balls stand for Na^+ cations. The octahedra represent [MnO_6] with some oxygen atoms being shown for clarity.

birnessite under our experimental conditions. However, when NaCl (or other sodium salts) is replaced with NaOH, the transformation of Na−birnessite to Na−2 × 4 did not occur. The reason for this is not clear.

2. Crystal Structure. Synthetic Na−2 × 4 materials are nanofibrous crystals (~60 nm × 20 nm × 20 μm). The crystal grows along the *b* direction, the tunnel direction. Like other 2 × *n* families of tunnel structure manganese oxides, such as Hollandite (2 × 2), Romanechite (2 × 3), RUB-7 (Rb−2 × 4), and Rb−2 × 5, Na−2 × 4 is also a mixed valent manganese oxide. On the basis of elemental analysis and the average oxidation state of manganese, the formula of Na−2 × 4 can be written as $Na_{0.33}Mn^{3+}_{0.33}Mn^{4+}_{0.67}O_2{\cdot}xH_2O$. The unit cell parameters (*a*, *b*, *c*, and β) for Na−2 × 4 are 14.434(5) Å, 2.849(7) Å, 23.976(6) Å, and 98.18°, respectively. Compared to the unit cell parameters of Rb−2 × 4 (RUB-7), which are $a = 14.191(3)$ Å, $b = 2.851(1)$ Å, $c = 24.343(7)$ Å, and $\beta = 91.29(2)°$, the *a* axis of Na−2 × 4 is longer than that of Rb−2 × 4 and the *b* axis of Na−2 × 4 is shorter than that of Rb−2 × 4. The β value of Na−2 × 4 is larger than that of RUB-7. These facts suggest that $Mn^{3+}O_6$ octahedra might be located in the double-chain sites rather than in the edges of quadruple chain sites as they are in Rb−2 × 4 (see Figure 9). Because the X-ray diffraction peaks are relatively broad as a result of the nanofiberlike crystallinity of Na−2 × 4, structural Rietveld refinements are difficult.

3. Thermal Stability and CO_2 Adsorption. TGA (Figure 5a) and TPD (Figure 6a) data show that Na−2 × 4 materials are thermally stable up to 450 °C. In fact, the X-ray diffraction pattern of a Na−2 × 4 sample shows no significant changes after the sample was calcined at 450 °C for 7 days. These data indicate that at this temperature the phases did not change and oxygen was not released from the framework of Na−2 × 4 samples. The water peaks (at ~150 and ~245 °C, respectively) in the TGA profile of Na−2 × 4 reveal that there are at least two types of sites in which water molecules are present. Compared to the TGA profile of layered birnessite (Figure 5b), the peaks (adsorbed CO_2 ignored) at about 150 °C in the TGA profiles can be assigned to adsorbed water or loose interlayer water. The peak at 245 °C in the Na−2 × 4 TGA profile suggests that some water molecules must have been confined in the tunnels when the Na−birnessites were transformed into Na−2 × 4 materials. The removal of these water molecules does not affect the tunnel structure of Na−2 × 4. However, the interlayer spacing in Na−birnessite does change from 7.0 to 5.6 Å, corresponding to the loss of water when Na−birnessite samples were dehydrated.[28]

Peaks related to removed oxygen species in the TGA and TPD profiles of Na−2 × 4 indicate that several types of oxygen species were present in the Na−2 × 4 materials. Yin and co-workers have studied in detail oxygen species in synthetic manganese oxides with tunnel structures.[29,30] They suggested that there are three types of oxygen species that were labeled as α-, β-, and γ-species corresponding to oxygen released in lower temperature regions (LT), intermediate temperature regions (MT), and high-temperature regions (HT), respectively. The small amount of α-species was assigned to weakly bound chemisorbed oxygen species. The β- and γ-species were believed to be due to different structural oxygen species bound to manganese cations. This is the case for Na−2 × 4 materials. However, the temperature regions shifted to even higher values than those for OMS-1 and OMS-2. As has been discussed above, the tunnel structure of Na−2 × 4 still remained intact, even when the sample was heated at 450 °C for several days, because the very small amount of desorbed oxygen species was due to surface adsorption. When lattice oxygen was released from the framework in the higher temperature regions, the Na−2 × 4 phase no longer existed with the formation of new phases. The transformations of tunnel structure manganese oxides and the nature of the released oxygen species corresponding to calcined temperatures will be discussed in detail elsewhere.

A trace amount of CO_2 has been revealed from the TPD analysis of Na−2 × 4. In Figure 6a, two broad CO_2 peaks under 400 °C imply that CO_2 molecules are adsorbed on different sites. The CO_2 TPD profile of Na−2 × 4 is similar to those of Na−birnessite (Figure 6b) and other tunnel structure manganese oxides synthesized from Na−birnessites in basic media (such as OMS-1), but is different from synthesized manganese oxides prepared under acidic conditions, such as OMS-2 materials, whose CO_2 TPD profiles do not show any peaks at all (unpublished data). Although this article will not discuss the nature of the adsorptive sites on these manganese oxide materials, it can be concluded that Na−2 × 4 materials possess basic sites, as does OMS-1. The CO_2 absorbed on these materials might have been obtained directly from the atmosphere or introduced by trace CO_2 impurities dissolved in the NaOH solution during synthesis.

(28) Chen, R.; Zavalij, P.; Whittingham, M. S. *Chem. Mater.* **1996**, *8*, 1275.
(29) Yin, Y. G.; Xu, W. Q.; Shen, Y. F.; Suib, S. L. *Chem. Mater.* **1994**, *6* (10), 1805−1808.
(30) Yin, Y. G.; Xu, W. Q.; DeGuzman, R.; Suib, S. L. *Inorg. Chem.* **1994**, *33* (19), 4384−4389.

Acknowledgment. The authors thank the U. S. Department of Energy, Office of Basic Energy Sciences, Division of Chemical Sciences, for support of this research. We also thank Dr. Ying Ma for help collecting EXAFS data and Dr. Frank Galasso and Dr. Zi Gao for helpful suggestions.

CM000777R